Journal of the Serbian Society for Computational Mechanics / Vol. 14 / No. 2, 2020 / pp 14-30
(10.24874/jsscm.2020.14.02.02)

BIOMECHANICAL BEHAVIOUR OF THE TOTAL HIP PROSTHESIS SUBJECTED TO NORMAL GAIT CYCLE LOAD: IDENTIFICATION OF THE DAMAGE IN THE CEMENT MANTLE

Mohammed El Sallah Zagane[1], Ali Benouis[2,4], Abdelmadjid Moulgada [1,3]*, Nourredine Djebbar[4,5], Abderrahmane Sahli[4]

[1] University of Tiaret, BP 78, City ZaarouraTiaret 14000, Algeria
E-mail: mohammedelesallah.zagane@univ-tiaret.dz
[2] University of Moulay Taher Saida,BP 138, City Ennasr Saida 20000, Algeria
E-mail: alymouh1980@yahoo.fr
[3] University of Tiaret, BP 78, City ZaarouraTiaret 14000, Algeria
Laboratory LRI, University of Tiaret, BP 78, City Zaaroura, Tiaret 14000, Algeria
E-mail: amoulgada@hotmail.fr
[4] Laboratory of LMPM, University of Sidi Bel Abbes, BP 89, City Ben M'hidi, Sidi Bel Abbes 22000, Algeria.
E-mail: sahliabdrahmen@yahoo.fr
[5] Universite Hassiba Benbouali University of Chlef, 02000, Algeria
E-mail: djebbarnour@yahoo.fr
**corresponding author*

Abstract

Cement is the weakest link in the composition of total hip prosthesis in terms of mechanical properties. The knowledge of the intensity and distribution of stresses on the cement attaching the implant to the bone is of great importance for understanding the condition of the prosthesis and its failure. In this study, the finite element method is used to analyze the magnitude and the equivalent Von Mises stress distribution induced in different components of the total hip prosthesis (THP) as well as the identification of the damage induced in the cement and between two cavities located in the polymethyl methacrylate (PMMA). The crack propagation is determined and localized using the extended element method (XFEM). The results show that the fracture stress of the cement in its proximal part is very important. These stresses increase considerably with the interaction of the cavities in this binder, causing damage to the cement and the loosening of the prosthesis.

Keywords: Total hip prosthesis, finite element method, bone cement, stress, damage, XFEM.

1. Introduction

In orthopedic surgery, there is an important need for a material capable of improving the initial fixation of the implant. In addition, a material or technique is also required to facilitate the restoration and/or reduction of bone defects. The synthetic materials currently available present

a number of problems. The mechanical strength of the THP largely depends on the type of cement used. Audrey (2007) and Benbarek et al. (2009) proved that the main role of the cement is to ensure good bone-implant adhesion and homogenize the load transfer from the implant to cement to the bone.

The difference between the stiffness of the cement and bone is analyzed by Lee AJC (2000). The Young's modulus of the prosthesis total hip is hundred times that of cement and about ten times that of cortical bone. To ensure the bone is not damaged, the cement must act as an interface that absorbs the loads that can occur between the cement and the implant.

Ormsby et al. (2010) and Marrs et al. (1997) made various studies in which they have changed the composition cements and have achieved significant reductions in the maximum temperature attained during hardening and significant changes in some of their characteristics, such as mechanical strength or fatigue behavior.

Initially, the only method of material preparation was mixing of the cement powder and monomer by hand. This resulted in an unpredictable porous material with average porosity levels varying from four to 13%. Lewis (1997) said porosity arises because of entrapped air, evaporation of the monomer component, incomplete filling of the bone cavity is proving by Culleton et al. (1993), investigation of Gilbert et al. (2000) premature solidification and polymerization shrinkage of the cement. Given bone cement's susceptible to fatigue failure in vivo, the presence of stress concentrations in the form of porosity became an area of considerable focus.

Hoey et al. have found (2009) the effect on stress concentration is dependent on size and distribution pore in the cement. In a recent study the present authors examined the pore size distributions in Hand-Mixed (HM) and Vacuum-Mixed (VM). Manual mixing of cement leads to know areas that are exposed to significant levels of damage to the cement and this risk is more likely an implanted limb could be perceived as a reimplantation or a prosthetic member as stated here. Foucat (2003) and Bachir Bouiadjra et al. (2007), after their investigation said this is to provide areas where the damage in the cement is concentrated.

Bachir Bouiadjra et al. (2007), according to their analysis, proved that the crack propagation can lead to the cement mantle fracture and subsequently loosening of the prosthesis. One factor that could affect the fracture toughness is porosity, as some investigators have suggested by Vila et al. (1999), Since pores have been identified in vitro as stress-raisers and crack-initiators were proved by Topoleski (1993), Bhambriet al. (1995) and McCormack et al. (1999) investigated that the higher degrees of porosity may contribute to micro-cracking. Ouinas et al. (2009) according to their research, prove that the mechanical resistance of the total hip prosthesis and particularly the adhesion quality between the implant and the bone depend primarily on the nature of cement used and its mechanical and geometrical characteristics and cement must withstand the subjected mechanical stresses; which may lead to the creation and propagation of cracks, and to the damage of the whole THP structure. The failure behavior of the fixation interface is ascribed to the initiation and propagation of cracks from defects along the bonded surfaces between cement and bone is investigated by Bouziane et al. (2010).

Benouis et al. (2015) analyzed the mechanical behavior of cracks initiated in the cement mantle by evaluating the SIFs. The effect of the defect on the crack propagation path was highlighted. Zagane et al. (2016), compared the fractures predicted using different material properties (Isotropic/Orthotropic) and loads (resembling different falls). Fracture behavior modeling of a 3D crack emanated from bony inclusion in the cement PMMA of total hip replacement Cherfi et al. (2018). Bachir Gasmi et al. (2019) studied the effect of the presence of different shapes and positions of micro-cavities on the crack initiation risk and its site in the orthopedic cement using the Extended Finite Element Method (XFEM). This study predicts the cracks propagations paths for all initiated cracks.

This study was carried out in order to understand and observe the phenomena of damage in the weakest element of THP, and due to the interaction of the defects observed experimentally (Fig.1).

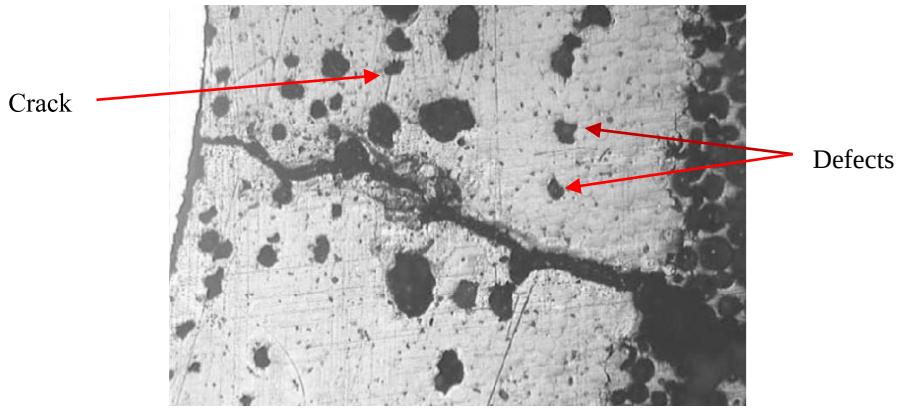

Fig. 1. Crack detection and cavity (magnification, 100x) in the cement bone. (Katzer, et al. 2007).

2. Finite element modeling

2.1 Geometric model

The obtaining of the 3D model of the femur is done by taking images of the interesting regions using the medical imaging technique (CT-scan). The thickness of each slice is about 1 mm for the proximal part until the small trochanter and 8mm from the small trochanter to the most distal of the shaft. The Charnley-Muller-Kerboul third generation (CMK3) prosthesis is designed using the Solidworks Software and includes the assembly of all parts of the prosthesis into one CAD model. To analyze the behavior of cement pores, a three-dimensional model of the total hip prosthesis was developed. This model is composed of a femoral stem, cement, cancellous and cortical bone (Figure 2). The interfaces between implant-cement and the different components of the THP are considered as continuous rigid.

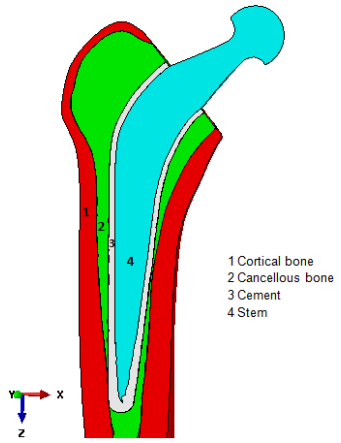

Fig. 2. Longitudinal section of the reconstructed prosthesis and their components

2.2 Material properties

The mechanical characteristics of the cancellous bone and cortical bone components of the model are shown in Table 1.

The cortical bone is considered as a transversely isotropic elastic material, whereas the spongy bone, cement and Charnley stem, are considered as linear isotropic elastic materials.

Bone cement is made of the polymer that has a relatively low Young's modulus, it has a bad resistance to tensile loading (Tensile strength = 25 MPa, compressive strength = 80 MPa (Rodriguez et al. 2014) and the shearing strength = 40 MPa) (Merckx et al.1993).

In other words, it is less stiff. Hence, when the hip prosthesis is loaded, it will transfer some of the load to the cortical through bone cement.

Part of Model	*Elastic Modulus (GPa)*	*Poisson's Ratio*
Stem (Ti-6Al-4V)	*210*	*0.3*
Cement	*2.4*	*0.3*
Cancellous bone	*0.4*	*0.3*
Cortical bone	*Ex,Ey=7.0, Ez=11.5 Gxy=2.6, Gyz, Gzx=3.5*	*Nxy= vzy=vzx=0.4*

Table 1. Material properties of femur THR (Daan et al. 2012)

2.3 Loading and boundary condition

In this study, for static and dynamic analysis, a load is applied on the surface of the implant bearing as shown in Fig. 3. Static load represents a person of 70 kg (Table 2), this load analysis is based, by selecting the peak load during the normal walking activity.

Force (N)	F_X	F_Y	F_Z
Joint contact force	*-433.8*	*-263.8*	*-1841.3*
Abductor muscle	*465.9*	*34.5*	*695.0*
Vastus Lateralis muscle	*-7.2*	*148.6*	*-746.3*

Table 2. Maximum loading configurations of the major muscles (Bergmann et al. 2001)

For the static analysis, the effort of the abductor muscle was simulated by a load applied to the proximal area of the greater trochanter ($F_{abductor}$), and the Vastus Lateralis load applied at the quadriceps tendon attaching via the patella to the tibial tubercle. The applied static forces are provided in Table 2, as are the forces imposed on the proximal femoral part.

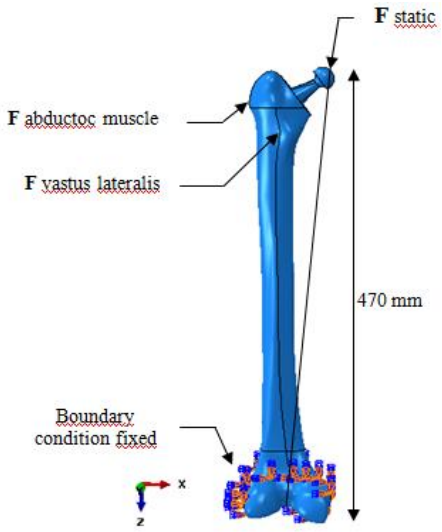

Fig. 3. Applied forces on the bone prosthesis and boundary conditions

For dynamic loads from the normal walking activity was chosen from the hip contact forces, these loads for a person of 70 kg are illustrated in Fig. 3.

The boundary condition was applied by fixing the distal epiphysis, which is the distal end of the femur that is connected to the knee (Behrens et al. 2009). We analyzed the mechanical behavior of cement during the process of normal walking of the patient; which the decomposition cycle is illustrated in Figure 4.

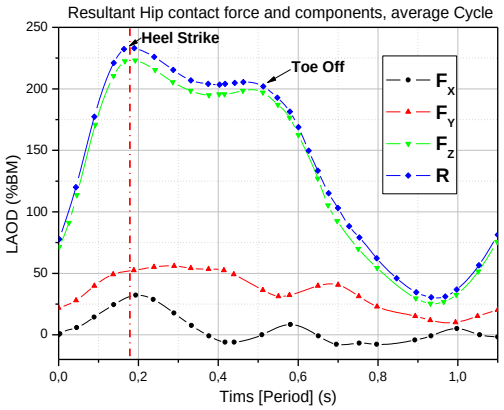

Fig. 4. The variation of forces applied on the prosthesis during normal walking. Contact force F and its components -Fx; -Fy; -Fz: F and -Fz are nearly identical. For BW = 70 kg. (Bergmann et al. 2001).

2.3 Model mesh

Numerical simulation of this behavior was performed using Abaqus 6.17 (Dassault Systèmes, RI, USA). The structure was meshed tetrahedral quadratic element (C3D10), constituting the following: Cement: 90822; Cortical bone: 286392; Cancellous bone: 275203; and Implant: 24096 elements. As shown in Figure 5.

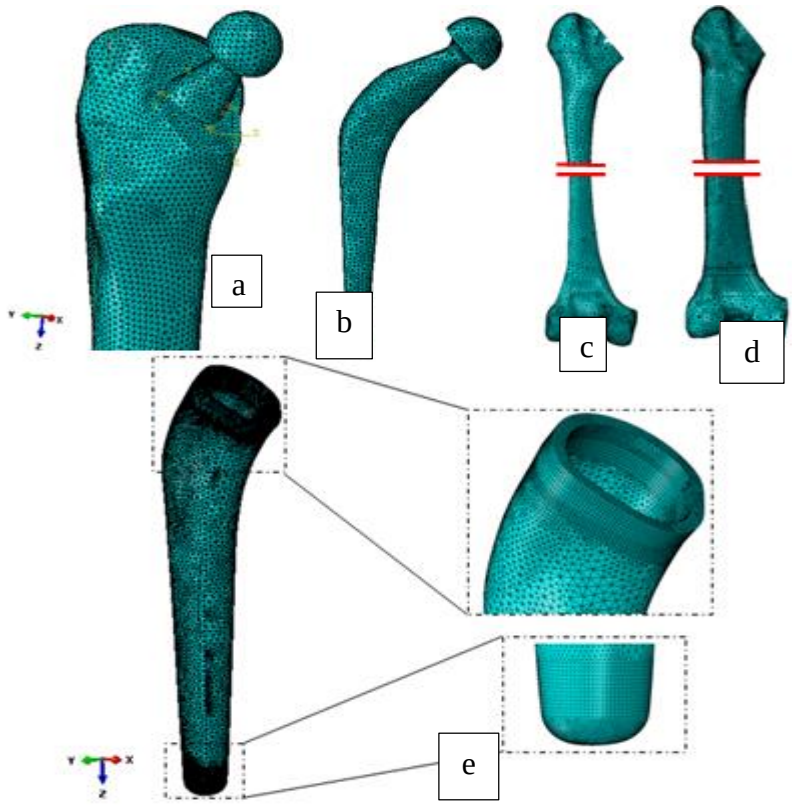

Fig. 5. Finite element meshes of the different parts of the hip prosthesis (a), implant (b), Cancellous bone (c) and Cortical bone (d), with refined meshing of the proximal region of the cement (e).

The mesh of the cement around the cavity at the interface with cavity and cement and inter distance between two cavities. The spherical micro-cavity with 0.2 mm of diameter is supposed to exist in the cement mantle (proximal and distal parts) are shown in Figure 6.

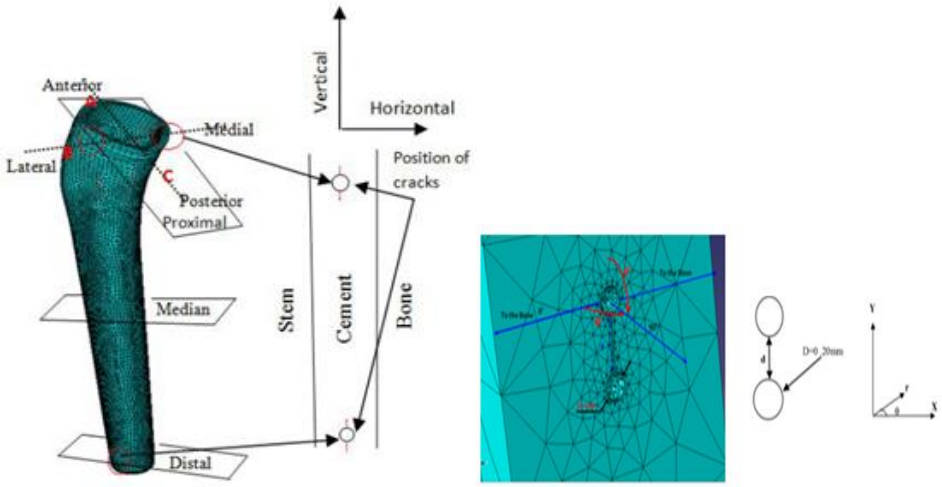

Fig. 6. Mesh around two-cavities in the cement.

3. Results and discussions

3.1 Stress distribution in the cement

Figure 7 clearly shows that the highest stresses are induced in the proximal cement. In this area, the cement is the most high mechanically solicited. The other two areas, the anterior and the lateral regions, are under low stress. The presence of a defect (cavities, blood bag or bone fragments) in this area of the cement is detrimental to the stability of the total hip prosthesis. By observing Figs. 7, it is found that, in the quasi-static and in heel strike, the von Mises stress is still predicted to be high at proximal and distal regions of the cement. Generally, the stresses in the cement in the heel strike from the working normal activity are higher (the maximum stress is in the order of 18 MPa), while the stresses on the cement of the quasi-static load are high (the maximum stress is in the order of 31 MPa).

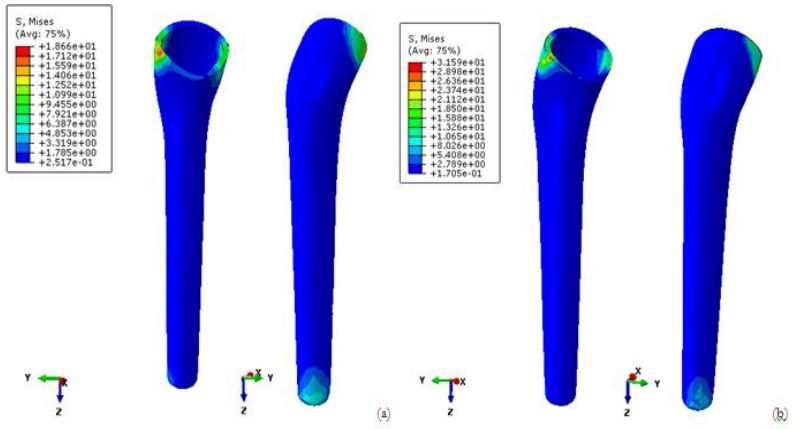

Fig. 7. Von Mises stresses distribution on the cement. (a): dynamic load (b): static load

3.2 Cortical bone

The Von Mises stress distributions within the femur bone is shown in Fig.8. It is found that the stress is still predicted to be high at the anterior and posterior area, whereas the minimum stress is always found to be at the distal end of the femur. Compared to the stresses, generally the stresses on the cortical bone in heel strike are higher (the maximum stress is the order of 153 MPa). But in the heel strike from the working normal activities are higher (the maximum stress is in the order of 387 MPa).

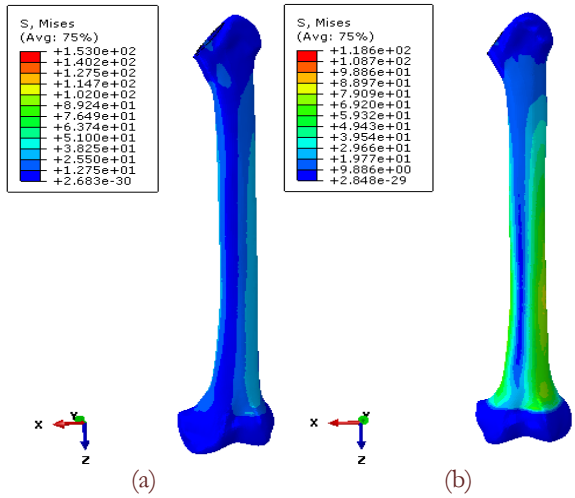

Fig. 8. Von Mises stresses distribution in the cortical bone. (a): dynamic load (b): static load

3.3 Cancellous bone

The Von Mises stress distributions within the cancellous bone is shown in Fig.9. It is found that the stress is still predicted to be high at the anterior and posterior area, whereas the minimum stress is always found to be at the distal end of the femur by quasi-statics load (the maximum stress is the order of 2 MPa). Compared to the stresses of the latter, the stresses in heel strike are higher (is the order of 4 MPa).

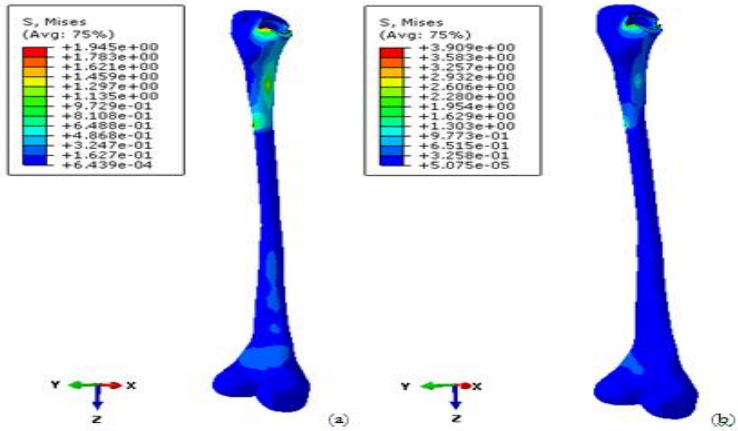

Fig. 9. Von Mises stresses distribution in the cancellous bone. (a): dynamic load (b): static load

3.4 Stem

Figure 10 show the von Mises stress distributions within the implant. Comparing the stress distributions on the hip prostheses, it can be observed that the stress concentration will be always at the neck area and the anterior and posterior zone. Again, this is reasonable since there are cross section transitions at the neck area and it should always exhibit high stresses there. The higher stress is found in the prosthesis that occurred under in heel strike.

The maximum stress is below 318 MPa. If it compares to the yield strength of stem is 427 MPa, there is still a safety factor of more than 2. Therefore, this result is still in the acceptable range.

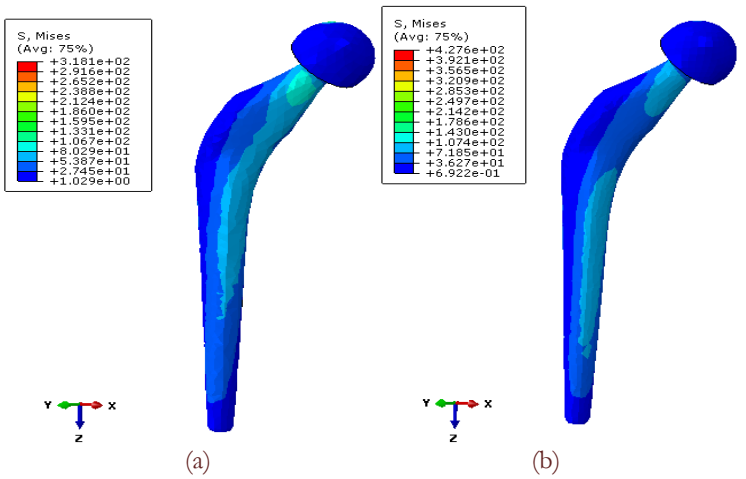

Fig. 10. Von Mises stresses distribution on the Stem. (a): dynamic load (b): static load.

4. Stress distribution around the pores

The location of the von Misses stresses can be observed in Table 3. It can be noticed that the nodes were the max and min. stresses are located in exactly the same node in the interaction point between two cavities.

In below study we admit the lateral proximal part.

		Static		Dynamic
Inter distance Position		d=0.2mm	d=0.005mm	d=0. 005mm (in heel strike)
Van Misses Stress	Medial part	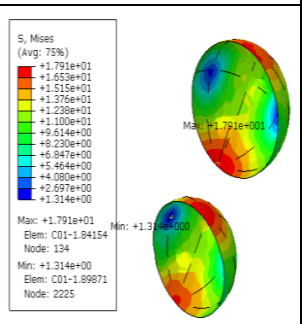	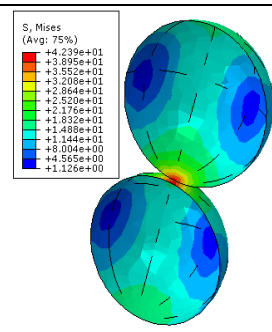	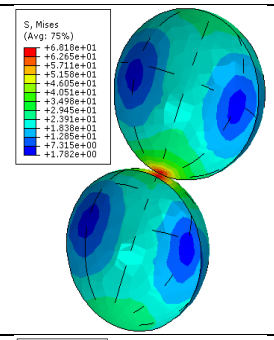
	Lateral Part	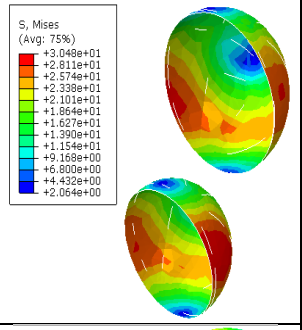	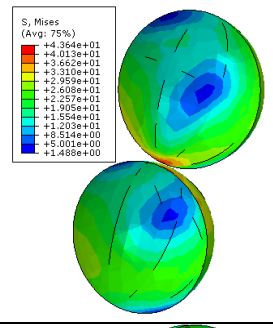	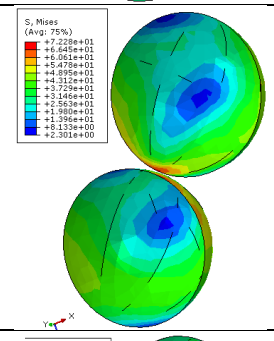
	Distal part	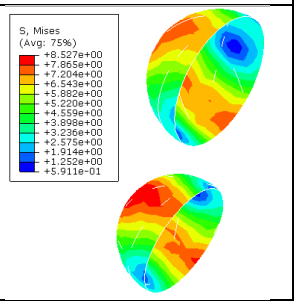	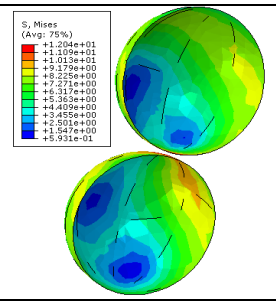	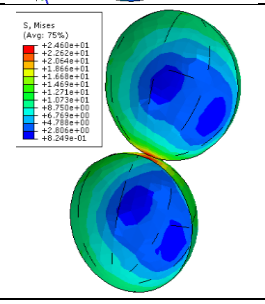

Table 3. Von Mises stresses distribution in the different zones on the inter-porosity distance in bone cement.

5. Spherical Stress distribution around the pores

5.1 Radial stresses (σ_{rr})

Fig. 11(a, b) presents the distribution of the radial stresses for different angles around the micro-void for the proximal zones. The danger of rupture of the cement mantle is not important according to the radial direction for the other region, since the stresses on the cement around the micro-cavity are very weak. In the proximal region the radial stresses lie between 4 MPa in the angle 90° and -7,7 MPa in the angle 0° to change between 4MPa in the angles 135°, 157° and -8MPa in the angle 45° respectively in the inter-distance 0,1mm and 0,02mm. At the interaction

point the stress augments from -3MPa to -5MPa. Thus the cement with the micro-void nearly is subjected to compressive stresses. One can conclude that there is no risk of fracture in this region because the cement, in general, has a good resistance to compressive loading.

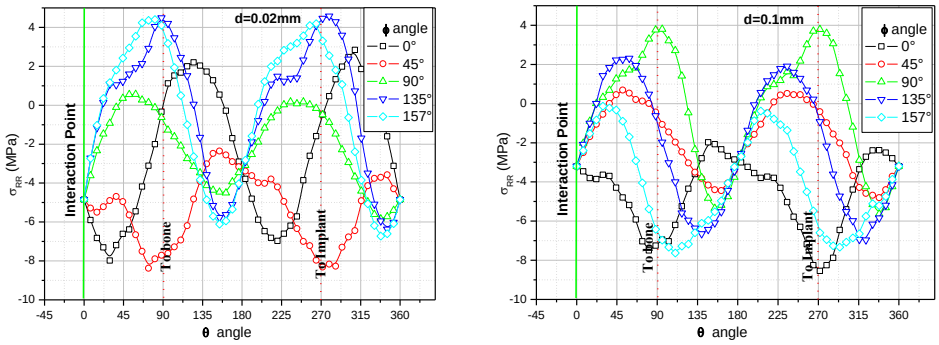

(a) micro-void, d=0.02 (b) micro-void, d=0.01

Fig. 11. Distribution of radial stresses (σrr) around micro-void (a) d=0.02, (b) d=0.1.

5.2 Circumferential stresses ($\sigma_{\theta\theta}$)

Fig. 12 (a, b) presents the distribution of the angular stresses for different angles around the micro-void in the proximal position case. One notices that the angular stresses $\sigma_{\theta\theta}$ are more important than the radial stresses σrr. This is due to the moment of rotation generated by the application of the load F. Consequently, the risk of the fracture of the cement mantle is very important according to the angular direction. The highest principal angular stress in the cement mantle occurred around the micro-void which to locate in the angle 90° to change in the angle 135° respectively in niter-distance 0.1mm and 0.02mm, the stress level is very important, they can reach 11.3 MPa when the angle was 135°.

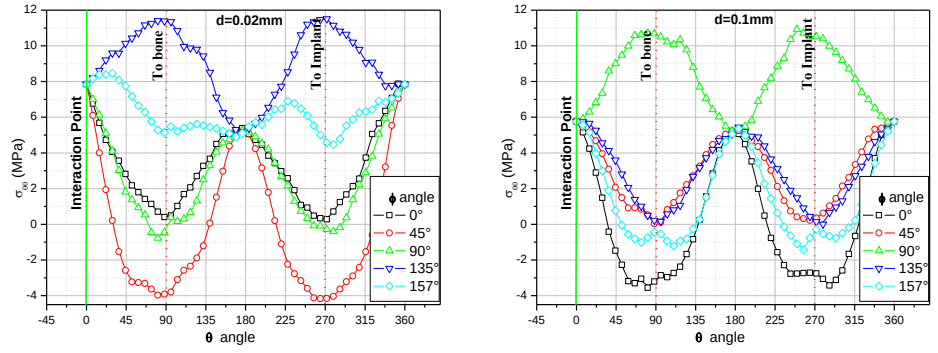

(a) micro-void, d=0.02 (b) micro-void, d=0.01

Fig. 12. Distribution of *Circumferential* stresses ($\sigma_{\theta\theta}$) around micro-void

5.3 Shear stresses ($\sigma_{r\theta}$)

Fig. 13 (a, b) presents the distribution of the Shear stresses for different angles around the micro-void in the proximal region. The micro-void situated in the proximal part can create a risk of the rupture of the cement mantle by shearing. The cement in general, does not resistant to shearing load well. The maximum stress value is about 7.5 MPa, it is noted that the shear stresses at the interaction point lie between 4.3 and 6 MPa in inter-distance 0.1mm and 0.02mm compared to other study (Topoleski et al. 1993).

The risk of the fracture of the cement of shearing is then lower. From a big inter-porosity distance the risk is practically non-existent.

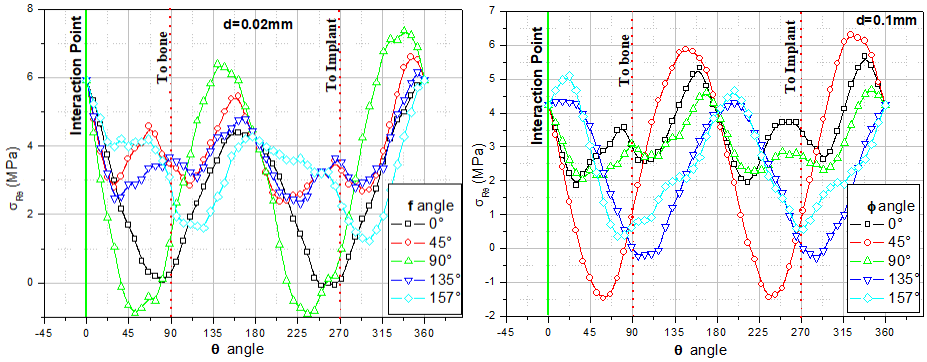

(a) micro-void, d=0.02 (b) micro-void, d=0.01

Fig. 13. Distribution of *shear* stresses ($\sigma_{r\theta}$) around micro-void

6. Identification of the damage in the cement mantle

6.1 Stage of Simulation damage in the cement, implementing Extended Finite Element Method.

The break is between 0.3 and 0.5 ms and corresponds to the second peak stress on curves. The distribution of the Von Mises stress is the same until the break but changes afterwards.

Figure 14 shows the simulation results with the X-FEM we detected the crack initiation in the cement in the proximal lateral where the concentrated stress. This figure clearly shows the damage criterion reliability, because the damaged zone emanates from the micro cavity where the area of the higher stress gradient and the corresponding area can be assimilated to emanate crack from the cavity with a length which could be measured.

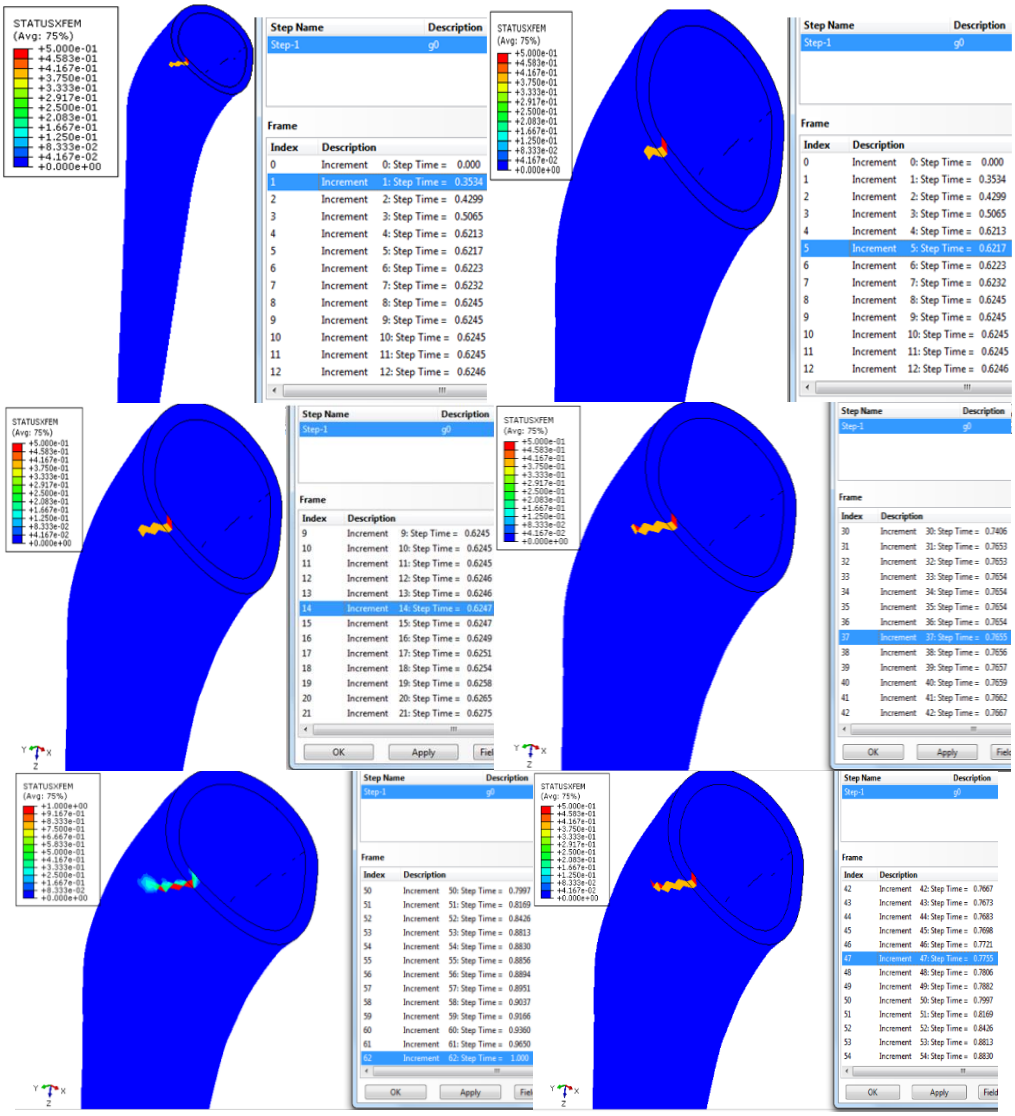

Fig. 14. Crack evolution at different increment in the cement.

Figure 15 represents the damaged area in the cement in the vicinity of the interconnection distance cavity. We can notice the presence of the damaged area (red) on the tip of this area, we can notice a stress concentration. This figure shows a resemblance to that of a stress concentration around an adjacent micro-cavity, so we can approximate our damaged area to multi-cracks.

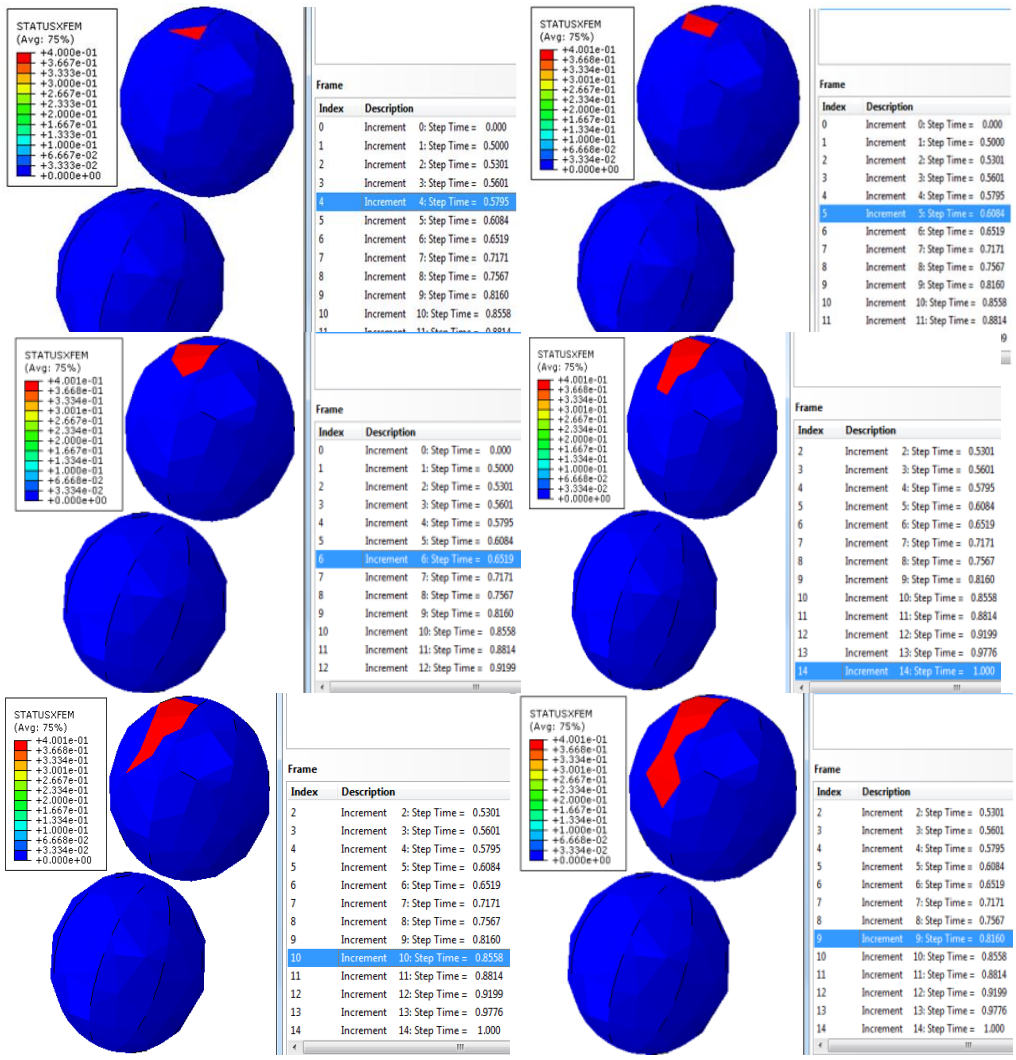

Fig. 15. Crack evolution at different increment in the cement between tow cavities.

Conducting numerical calculations considering the damage process of model components' material structure as well as connections between the application of suitable numerical proceedings containing parameters describing the mechanism of damage formation and propagation. The Extended Finite Element Method (XFEM) is a technique applied to simulate crack initiation and propagation in the model.

A basic constitutive law used for describing the damage process in Abaqus /Standard software is Traction–Separation.

In both cases, elastic material with parameters characterizing material damage was defined as follows: Young's modulus E =2400 MPa, Poisson's ratio ν = 0.3, value of stress initiating damage of the cement σmax = 25 MPa.

According to the modeling of our model by the XFEM method of the cavity and orthopedic cement, there is initiation of the damage in the lateral part of the cement, because of the stresses, which are very high in this part, due to the very high loading imposed on the implant towards the cement.

The most important damage in the cement is located in the proximal lateral zone (compression stress) and with two cavities; it is caused by compression of the cement in the radial direction around the cavity. An implant inclination generates damage with different states and levels; the more interconnection of the cavity is low the more the damage zone is greater.

7. Conclusion

The results obtained in this work show that:

In the cement mantle the critical region is still predicted to be in the neck region of the hip total prosthesis. The critical stress is much lower than the yield strength. Hence, the design of the prosthesis is believed to be safe for use.

Compared to the proximal part, the distal region of the cement is subjected to the stress of low amplitude.

The presence of the cavity in the bone cement is the source of an additional stress of the notch effect.

The higher the Von Mises stresses induced in an empty cement of the cavities are located on the lateral proximal part.

The most important damage in the cement is located in the proximal medial zone (compression stress).

The interconnection of the cavities increases the possibility of damaging the cement.

References

Audrey P H (2007). Elaboration d'un modèle mécanique de l'articulation de la hanche sous sollicitations dynamiques–Application à l'étude de l'influence d'une orthèse podale sur une hanche arthrosique (Doctoral dissertation).

Bachir Bouiadjra B, Belarbi A, Benbarek S, Achour T, Serier B (2007). Analysis of the behaviour of microcracks in the cement mantle of reconstructed acetabulum in the total hip prosthesis Original, *Comp. Mater. Sci*. 40 (4) 485-491.

Behrens BA, Ingo N, Wefstaedt P; Stukenborg-Colsman C; Bouguecha A (2009). Numerical investigations on the strainadaptive bone remodelling in the periprosthetic femur: Influence of the boundary conditions, *BiomeEng*, Online. 7.http://dx.doi.org/10.1186/1475-925X-8-7

Benbarek S, Bouiadjra BB, Mankour A, Acour T & Serier B (2009). Analysis of fracture behaviour of the cement mantle of reconstructed acetabulum. *Computational materials science*, 44(4), 1291-1295.

Benouis A, Boulenouar A, Benseddiq N and Serier B (2015). Numerical analysis of crack propagation in cement PMMA: application of SED approach. *Structural Engineering and Mechanics*, Vol. 55, No. 1 93-109 DOI: http://dx.doi.org/10.12989/sem.2015.55.1.093.

Bergmann G, Graichen F, and Rohlmann A (1993). Hip Joint Loading During Walking and Running, Measured in Two Patients. *J.Biomech*, vol. 26, pp. 969–990.

Bergmann G, Deuretzbacher G, Heller M, Graichen F, Rohlmann A, Strauss J and Duda GN (2001). Hip contact forces and gait patterns from routine activities. *Journal of biomechanics*, 34(7), 859-871.

Bhambri SK and Gilbertson LN (1995). Micro mechanisms of fatigue crack initiation and propagation in bone cements. *J. Biomed. Mater. Res*, 29, 233–237.

Bouziane MM, Bachir Bouiadjra B, Benbarek S, Tabeti MSH, Achour T (2010). Finite element analysis of the behaviour of microvoids in the cement mantle of cemented hip stem: Static and dynamic analysis. *Materials & Design*, 31, 545–550.

Cherfi M, Abderahmane S and Benbarek S (2018). Fracture behavior modeling of a 3D crack emanated from bony inclusion in the cement PMMA of total hip replacement. *Structural Engineering and Mechanics*, Vol. 66, No. 1, 37-43 DOI: https://doi.org/10.12989/sem.2018.66.1.037.

Culleton T P, Prendergast P J, Taylor D (1993). Fatigue failure in the cement mantle of an artificial hip joint. *Clinical Materials*; 12:95–102.

El-Sheikh HF, MacDonald J B, and Hashmi MSJ (2002). Material Selection in the Design of the Femoral Component of Cemented Total Hip Replacement. *J. Mater. Process Technology*, vol. 122, pp. 309–317.

Foucat D. (2003). *Effet de la présence d'un grillage métallique au sein du ciment de descellement de prothèse totale de la* hanche *(étude mécanique et thermique)*, Thèse Université Louis Pasteur, Strasbourg I.

Gasmi B, Abderrahmene S, Smail B, and Benaoumeur A (2019). Initiation and propagation of a crack in the orthopedic cement of a THR using XFEM. *Advances in Computational Design*, 4(3), 295-305.

Gilbert J L, Hasenwinkel J M, Wixson R L, Lautenschlager P (2000). A theoretical and experimental analysis of polymerization shrinkage of bone cement: a potential major source of porosity. *Journal of Biomedical Materials Research*; 52:210–8.

Hoey D and Taylor D (2009). Quantitative analysis of the effect of porosity on the fatigue strength of bone cement. *Acta Biomaterialia* 5(2):719–26.

Katzer A, Ince A, Hahn M, Morlock M M and Steens W (2007). Cement mantle defects in total hip arthroplasty: influence of stem size and cementing technique. *Journal of Orthopaedics and Traumatology*, 8(4), 167-172.

Lee AJC. (2000). The time-dependent properties of polymethylmet-hacrylate bone cements: the interaction of shape of femoral stems, surface finish and bone cement. Learmonth I. D (ed.). *Interfaces in total hip arthroplasty*. London: Springer – Verlag Ltd. P. 11-9.

Marrs B H (2007). *Carbon nanotube augmentation of a bone cement polymer* [thesis doctoral], University of Kentucky.

McCormack B.A.O, P.J. Prendergast. (1999), Microdamage accumulation in the cement layer of hip replacements under flexural loading. Journal of Biomechanics, Volume 32, Issue 5, Pages 467-475.

Merckx D (1993). Les ciments orthopédiques dans la conception des prothèses articulaires. Biomécanique et biomatériaux, Cahiers d'enseignement de la SOFCOT, *Expansion scientifique française*, 44, 67–76.

Ouinas D, Bachir Bouiadjra B, Serier B, Benderdouche N, Ouinas A (2009). *Comput. Mater. Sci*., 45, 443–448.

Rodriguez. Lucas C, Chari. Jonathan, Gindri. ShantAghyarian, Izabelle M, Kosmopoulos. Victor, and Rodrigues. Danieli C. (2014). Preparation and Characterization of Injectable Brushite Filled-Poly (Methyl Methacrylate) Bone Cement, *Materials*, 7, 6779-6795.

Topoleski L D T, Ducheyne P, Cuckler J M, (1993). Microstructural pathway of fracture in polymethylmethacrylate bone cement. *Biomater*, 14(15), 1165–1172.

Waanders D, Janssen D, Kenneth M A, and Verdonschot N (2012). The behavior of the micro-mechanical cement-bone interface affects the cement failure in total hip replacement. *J Biomech*. Author manuscript; available in PMC January 11.

Zagane M S, Benbarek S, Abderahmane S, Bachir Bouiadjra B and Boualem S. (2016). Numerical simulation of the femur fracture under static loading, *Structural Engineering and Mechanics*, Vol. 60, No. 3 405-412 DOI: http://dx.doi.org/10.12989/sem.2016.60.3.405.